Genetic-algorithm-aided meta-atom multiplication for improved absorption and colouration in nanophotonics

Changxu Liu,[†,‡] Stefan A. Maier,[*,‡,¶] and Guixin Li[*,†,§]

†*Department of Materials Science and Engineering, Southern University of Science and Technology, Shenzhen 518055, China*

‡*Chair in Hybrid Nanosystems, Nanoinstitute Munich, Faculty of Physics, Ludwig Maximilians University of Munich, 80539 Munich, Germany*

¶*Department of Physics, Imperial College London, London SW7 2AZ, United Kingdom*

§*Shenzhen Institute for Quantum Science and Engineering, Southern University of Science and Technology, Shenzhen 518055, China*

E-mail: stefan.maier@physik.uni-muenchen.de; ligx@sustc.edu.cn

Abstract

For a repertoire of nanophotonic systems including photonic crystals, metasurfaces and plasmonic structures, unit cell with a single element is conventionally used for the simplicity of design. The extension of the unit cell with multiple meta-atoms drastically enlarges the parameter space and consequently provides potential configurations with improved device performance. Simultaneously, the multiplication does not induce additional complexity for lithography-based fabrications. However, the substantially increased number of parameters makes the design methodology based on physical intuition and parameter sweep impractical. Here, we show that expanding the number of meta-atoms in the unit cell significantly improves the performance of nanophotonic

systems, by the virtue of a genetic algorithm based optimiser. Our approach includes physical intuition endowed in the geometry of meta-atoms, providing additional physical understanding of optimisation process. We demonstrate two photonic applications, including prominent enhancement of a broadband absorption and enlargement of the colour coverage of plasmonic nanostructures. Not limited to the two proof-of-concept demonstrations, this methodology can be applied to all meta-atom based nanophotonic systems including plasmonic near-field enhancement, nonlinear frequency conversion, as well a simultaneous control of phase and polarisation for metasurfaces.

KEYWORDS: plasmonics, nanostructure, structural colour, absorption, genetic algorithms

Introduction

The unit cell, a concept firstly coined in crystallography as the smallest group that can constitute the whole structure, is regularly transferred to photonics as the basic element for functionality. With the ability to manipulate and precisely tailor micro- and nanostructures, meta-atoms comparable to or smaller than the wavelength of light are achieved with unique optical properties beyond those offered by natural materials, in analogy with the angstrom-sized atoms that impact the behaviour of electrons in crystals. By extending the unit cell in certain ways (directly replicating or replicating after resizing/rotating), various nanophotonic platforms including plasmonics,[1] photonic crystals[2] and metamaterials[3] are realised, offering a plethora of applications ranging from lasing,[4,5] optical sensing,[6,7] colouration,[8] harmonic generation[9,10] to wavefront manipulation and energy harvesting,[11,12] to name a few.

For a large portion of photonic systems, unit cell with a single meta-atom is naturally chosen, by virtue of the widely-used design methodology based on *a priori* understanding of its electromagnetic response. A library of simple, physically intuitive building blocks such as disks, rings, rods with limited parameters is utilised, not only to realise the desired function but also to unveil the physics through the dependence between the limited variables and

certain measurable outputs by parameter sweeps. A unit cell with multiple meta-atoms could exponentially enlarge the size of the parameter space, driving the conventional design a formidable task.

On the other hand, from the perspective of nanofabrication, the expansion of the unit cell with multiple meta-atoms with different sizes (as shown in Fig. 1) introduces negligible additional cost, regarding standard top-down lithography based techniques including photolithography, ion beam lithography or 3D laser printing. The drastically enlarged parameter space induced by multiplication provides possibilities of a better design with improved figures-of-merit (such as the transmission efficiency, absorption, broadband responses and the quality factor) compared with structures consisting of unit cells with a single meta-atom. A design method for photonic systems with multiple meta-atoms is of widespread scientific and technological interest, considering the performance is one of the most critical factor to bridge the gap between proof-of-concept demonstration and practical applications. However, the enlarged parameter space makes physical "intuition" based design a daunting task.

Artificial intelligence (AI) brought promise to many areas of data-intensive research fields, including materials design,[13,14] recognition of phases of matter,[15,16] unconventional electronic logic gate[17,18] and quantum computing.[19,20] The recent surge of interest in AI-assisted photonics[21–43] enables optical design with a large number of degrees of freedom, including meta-atom multiplication. Recently, the idea of meta-atom multiplication was realised by unit cell composed of two separate meta-atoms with tunable geometrical parameters, for the manipulation of the polarisation and wavefront of light.[42] Here, we demonstrate that multiplication of identical-shaped meta-atoms with simple geometry are able to improve the device performance, taking advantage of the inter-atom coupling between meta-atoms. By utilising genetic algorithm (GA),[44] a metaheuristic algorithm widely used in optical design,[21–23,25–27,37–39] we apply the concept of meta-atom multiplication to two widely-investigated applications: broadband absorption and structural colour generation. We numerically implement the comparison before and after unit cell multiplication, demon-

strating an absorption enhancement from 79.2% to 93.4% through the whole visible and near-infrared, with both unextended and extended unit cells optimised by GA. For colour generation, the achievable area in the CIE diagram is enlarged by 106% for the extended unit cell.

The expansion of meta-atoms designed with physical intuition can not only provide optimal solutions, but also shed light on the further understanding of the optimisation. The idea of meta-atom multiplication can be feasibly applied to all meta-atom based nanophotonic systems if numerical methods can precisely predict the output. Meanwhile, other more advanced deep learning based algorithms such as generative adversarial networks,[40] semi-supervised learning,[43] convolutional neural networks,[33] bidirectional neural network[41] and hybrid artificial intelligence algorithm[42] could be utilised for improved optimisation.

Results and discussion

An efficient absorber at the micro or even the nano scale is particularly desired for energy harvesting, not only limited to photovoltaics,[11] but also for photo-thermal related applications[45] and photocatalysis.[46] Here, for simplicity, we choose a unit cell composed of a single metallic disk on a plasmonic mirror with a dielectric spacer between them. Both the meta-atom and the substrate are composed of gold, and the dielectric is selected as SiO_2 with refractive index $n = 1.45$. The period of the unit cell (T), the height (H) and the diameter (D) of the metal disk, the thickness (t) of the dielectric layer are parameters that can be adjusted for the optimal absorption in the spectral range with wavelength between 350nm and 800nm, a region which covers most of the solar energy. Linear polarised light is applied at normal incidence. GA is utilised as the optimiser for the maximum averaged absorption ($\bar{A}$). More details can be found in the Supporting Information 1.

Figure 2 summarises the results of GA-optimised absorption for unit cells with a single meta-atom. Figure 2a displays the progress of the optimisation process, illustrating the best

value (red diamonds) and averaged value (green diamonds) of $\bar{A}$ in each generation. To clarify the variation at high absorption, we apply a logarithmic scale in the y-axis, with the value of absorbance defined as $\bar{A}_{\log} = \log_{10} \frac{1}{1-\bar{A}}$. The best value of absorption increases with the number of generations, reaching a plateau after about 20 generations. The optimised value is achieved at 0.792, corresponding to an average of absorption of 79.2% from 350 to 800 nm. Figures 2b-e provide more details at different generations, with upper panels schematic cartoon of the configuration and lower panels the absorption spectra. The dashed-line in the absorption spectra refers to the averaged value. Parameters of each configuration can be found in Supporting Information 2. The variation of the configurations in Figures 2b-e may shed light on how to enhance the absorption for this simple structure. The distance between each disk is shortened to enhance the inter-particle coupling, while similarly the thickness between disk and metallic substrate is decreased for a stronger coupling. Combined with optimisation of the shape of the disk, the absorption is improved from 63.3% to 79.2%. However, a drastic degradation of absorption occurs for the wavelength larger 700nm (mainly due to the intrinsic material property of gold), which is undesirable for many solar energy-related devices.

For the next step, we extend the unit cell by doubling the period, generating four meta-atoms in each cell. Considering feasibility in planar nanofabrication, we select all four disks the same height. Besides the difference in diameters, each disk is located at different position, increasing the number of parameters from 4 to 15. Here, the deviation of meta-atoms from centre makes the inter-meta-atom coupling a parameter to optimise, playing a pivotal role in the improvement of device performance. This enlarged parameter space provides potential configurations with a further improved figure of merit (absorption).

Figure 3 demonstrates the results of GA-optimised absorption for multiplied meta-atoms, with Fig. 3a the relationship between absorption and generations and Fig. 3b-e details of configurations and absorption spectra of the best sample in selected generations. For a reasonable comparison, the optimisation process uses the same number of generations. The

parameters of each configuration can be found in Supporting Information 2.

A comparison between Figure 2a and Figure 3a directly elucidates the power of meta-atom multiplication for a better figure of merit. Both the averaged value and the best value in each generation is improved for the structures with extended unit cells. The optimised device achieves an averaged absorption of 93.4 %, with a 18% improvement compared to the case with single meta-atom. In Fig. 3b-e, more details of the optimisation process are provided. Figure 3b is a configuration with all the disks identical and the same inter-disk distance, which is equivalent to the configuration in Fig. 2b. As the GA process starts, the variations in size and position improve the absorption, as shown in Fig. 3c-e. Quite interestingly, we find a pair of touching disks in the configuration shown in Fig. 3c. This setup coincides with the prediction of transformation optics: the kissing point can provide broadband absorption.[47–49] Without *a priori* knowledge, the GA optimiser produces a geometric singularity to achieve a broadband response. However, the remaining two disks, especially the smaller one, need further optimisation. After some more generations, the absorption is improved as demonstrated in Fig. 3d. Although the configuration with a kissing point is not selected as the optimal case, the small distance among the disks greatly intensifies light-matter interaction, which can be explained by transformation optics.[50] Further, a small modification is done from Fig. 3d to Fig. 3e, improving the absorption from 89.4% to 93.4%. Two absorption peaks are observed at 710nm and 760nm, which ameliorate the absorption degradation in the case of unit cell without multiplication.

To obtain a better insight into the mechanism for the broadband absorption from GA, we implement additional numerical studies on the optimised configuration as depicted in the upper panel of Fig. 3e. The results are summarised in Fig.4. Figure 4a illustrates the absorption spectra with all four disks (upper panel), two disks (middle panel), single disk (lower panel), with the insets providing schematic views of the setups. The spectra are shifted along the y-axis for clarity. The lower panel of Fig.4a shows two setups with a single disk, where the inter-disk coupling is missing. With variation in disk size, adsorption peaks can

be produced around 620nm and 670nm, respectively. However, the absorption drops quickly in the near-infrared beyond 700 nm, agreeing with the investigation for unextended unit cells. When the two disks are brought together (middle panel), the absorption dramatically increases with a peak around 760nm (black dashed line), as a result of the coupling between the two disks.[50] By adding another two disks, the absorption is further enhanced, achieving a broadband response, as shown in the upper panel of Fig. 4a. Figures 4b-e illustrate the electric field distributions along y (E_y), while Figs. 4f-g demonstrate the absorption power density calculated as $P_{abs} = -\frac{1}{2}Re(\mathbf{E}\times\mathbf{H})$ for different configurations. Figure 4f combines the P_{abs} for Config.I-III. A comparison among Fig. 4b-d demonstrates the drastically enhanced electric field around disks induced by inter-particle coupling, which leads to the absorption enhancement illustrated in Fig. 4f. By introducing the additional two disks, the amplitude of E_y at near-field is further enhanced inside the unit cell, achieving an absorption of 96.1% at 760nm.

To demonstrate the generality of meta-atom multiplication as a guide for achieving better device performance, we utilise a similar method for structural colour generation. Compared to chemical-based colours, the colour generated from resonant interactions between light and metallic nanostructures provides an alternative way of colouration with advantages including better stability, improved pixel resolution and potential for sustainable production and recycling.[8] We ultilise the same configuration as used for broadband absorption. The aim is to design three unit cells that can generate three additive primary colours, red, green and blue separately. Again, we applied the GA to both the unit cell with a single meta-atom and the extended unit cell with four meta-atoms. We select the desired colours as three colours in the standard Red Green Blue (sRGB) colour space.[51]

We show the results for green colour generation in Fig. 5. Figure 5a illustrates the optimisation process for the best value in both cases with single meta-atom and multiple meta-atoms. Here, the distance Δ is the distance between the target colour (green) and the colour produced by the nanostructure in the CIE diagram. As generation increases, the

generated colour moves towards the destination for both cases. However, the extended unit cell reaches a much smaller Δ, corresponding to better colour purity. Figure 5b illustrates configurations and produced colours after GA optimisation. The left panel corresponds to the unextended unit cell with a single meta-atom while the right panel shows the one with multiple meta-atoms. A greenish colour cannot be obtained with only a single meta-atom. Figure 5c compares the corresponding reflection spectra. The additional disks embedded in the unit cell induce additional absorption of blue (around 400nm) and red (around 630nm) light, creating a purer green colour. Figure 5d depicts the CIE diagram inside the sRGB space, with the top vertex the desired colour. After meta-atom multiplication, the colour generated by meta-atom multiplication (black pentagram) is located much closer to the top vortex compared to the one with a single disk (black circle). A comparison with another optimisation algorithm, particle swarm, can be found in Supporting Information 2.

Similarly, we implemented the GA-based optimisation for the generation of blue and red colours; the details can be found in Supporting Information 3. Figure 6 summarises the available structural colours for the plasmonic structure with/without meta-atom multiplication in the CIE diagram. The sRGB space is enclosed in the white triangle. By utilising unit cell with a single disk, only 27.7% of the area of sRGB can be covered. Remarkably, the coverage rate increases to 57.0% by merely extending the unit cell with four disks, illustrating a 106% enhancement. The material property (stronger absorption at blue and reduced absorption at red) makes both the unextended/extended unit cells able to produce more precisely the stranded red colour. However, the extended unit cell can generate more reddish colour beyond the sRGB space, as shown in Supporting Information 3. This intrinsic feature also causes the deviation between the generated colours and standard blue. Nevertheless, a definite improvement is observed after meta-atoms multiplication.

To conclude, we propose a general methodology for improving the performance of nanophotonic systems operating on unit cells. A better figure of merit can be accomplished by extending the unit cell with multiple meta-atoms. Two proof-of-concept demonstrations of

broadband absorption and structural colour generation are presented. While systems with multiple meta-atoms have been reported,[23,24,42,52–54] we explicitly compare the performance between a unit cell with single meta-atom and the one with four meta-atoms, quantitatively demonstrating the advantages of meta-atom multiplication. Here we utilise genetic algorithm as a demonstration. Other more advanced algorithms recently developed in optics[33,40–43] could be used as the optimiser for faster and even better results. Considering negligible fabrication cost increase for more complexed patterns, it is interesting to further investigate larger unit cells (e.x. 3 by 3 elements instead of 2 by 2) and/or meta-atoms composed of different topologies for potential improvement in performance, by utilising more efficient optimisers or even replacing the Maxwell solver with an AI-based predictor.[33] More importantly, we believe that the idea of meta-atom multiplication can be applied to a plethora of photonic systems, such as plasmonic near-field enhancement, second/third harmonic generation, simultaneous control of phase and polarisation for metasurfaces. By multiplying simple elements with inter-element coupling, we may utilise the meta-atoms from physics intuition design as the basic element for extension. Not limited to an optimised solution, more in-depth understating of the mechanism can be gained through the investigation of optimised configurations, such as transformation optics.

As a proof-of-concept demonstration, we fixed the materials of unit cells. However, the material can also be parameterised in the optimiser for better results. For example, the optical properties for some dielectric materials makes them more feasible to generate blue colour than gold.[55] In demonstration, linearly polarised light is used for simplicity. In practical situations, polarisations along with other directions may also need to be counted in the optimisation process. In the optimised design shown above, there are some tiny features (such as two kissing disks or narrow gaps) which may not be easily achievable for some fabrication techniques. Additional constrain for the minimum inter-particle distance or merging closely located particles can be introduced for the ease of fabrication.

Acknowledgement

C. L. acknowledges the funding support from Humboldt Research Fellowship from the Alexander von Humboldt Foundation. S. A. M. acknowledges the funding support from the Deutsche Forschungsgemeinschaft (DFG, German Research Foundation) under Germany's Excellence Strategy, EXC 2089/1-390776260, the Solar Energies go Hybrid (SolTech) programme and Lee-Lucas Chair in Physics. G. L. is financially supported by National Natural Science Foundation of China (11874426 and 11774145), Guangdong Provincial Innovation and Entrepreneurship Project (2017ZT07C071).

Supporting Information Available

The following files are available free of charge.

- Additional information about the GA and FDTD simulations; detailed parameters for the optimised configurations; extra results of structure colour generation.

This material is available free of charge via the Internet at `http://pubs.acs.org/`.

References

(1) Maier, S. A. *Plasmonics: fundamentals and applications*, 1st ed.; Springer Science & Business Media: Berlin, Germany, 2007.

(2) Joannopoulos, J. D.; Johnson, S. G.; Winn, J. N.; Meade, R. D. *Photonic Crystals: Molding the Flow of Light - Second Edition*, 2nd ed.; Princeton University Press: Princeton, United States, 2008.

(3) Cai, W.; Shalaev, V. M. *Optical metamaterials fundamentals and applications*, 1st ed.; Springer: Berlin, Germany, 2010.

(4) Hess, O.; Pendry, J. B.; Maier, S. A.; Oulton, R. F.; Hamm, J. M.; Tsakmakidis, K. L. Active nanoplasmonic metamaterials. *Nature Materials* **2012**, *11*, 573.

(5) Ma, R.-M.; Oulton, R. F. Applications of nanolasers. *Nature Nanotechnology* **2019**, *14*, 12–22.

(6) Fenzl, C.; Hirsch, T.; Wolfbeis, O. S. Photonic crystals for chemical sensing and biosensing. *Angewandte Chemie International Edition* **2014**, *53*, 3318–3335.

(7) Brolo, A. G. Plasmonics for future biosensors. *Nature Photonics* **2012**, *6*, 709.

(8) Kristensen, A.; Yang, J. K.; Bozhevolnyi, S. I.; Link, S.; Nordlander, P.; Halas, N. J.; Mortensen, N. A. Plasmonic colour generation. *Nature Reviews Materials* **2016**, *2*, 1–14.

(9) Lapine, M.; Shadrivov, I. V.; Kivshar, Y. S. Colloquium: nonlinear metamaterials. *Reviews of Modern Physics* **2014**, *86*, 1093.

(10) Li, G.; Zhang, S.; Zentgraf, T. Nonlinear photonic metasurfaces. *Nature Reviews Materials* **2017**, *2*, 17010.

(11) Polman, A.; Atwater, H. A. Photonic design principles for ultrahigh-efficiency photovoltaics. *Nature Materials* **2012**, *11*, 174.

(12) Brongersma, M. L.; Halas, N. J.; Nordlander, P. Plasmon-induced hot carrier science and technology. *Nature Nanotechnology* **2015**, *10*, 25.

(13) De Luna, P.; Wei, J.; Bengio, Y.; Aspuru-Guzik, A.; Sargent, E. Use machine learning to find energy materials. *Nature* **2017**, *552*, 23–25.

(14) Curtarolo, S.; Hart, G. L.; Nardelli, M. B.; Mingo, N.; Sanvito, S.; Levy, O. The high-throughput highway to computational materials design. *Nature Materials* **2013**, *12*, 191.

(15) Carrasquilla, J.; Melko, R. G. Machine learning phases of matter. *Nature Physics* **2017**, *13*, 431.

(16) Van Nieuwenburg, E. P.; Liu, Y.-H.; Huber, S. D. Learning phase transitions by confusion. *Nature Physics* **2017**, *13*, 435.

(17) Bose, S.; Lawrence, C. P.; Liu, Z.; Makarenko, K.; van Damme, R. M.; Broersma, H. J.; van der Wiel, W. G. Evolution of a designless nanoparticle network into reconfigurable boolean logic. *Nature Nanotechnology* **2015**, *10*, 1048.

(18) Chen, T.; van Gelder, J.; van de Ven, B.; Amitonov, S. V.; de Wilde, B.; Ruiz Euler, H.-C.; Broersma, H.; Bobbert, P. A.; Zwanenburg, F. A.; van der Wiel, W. G. Classification with a disordered dopant-atom network in silicon. *Nature* **2020**, *577*, 341–345.

(19) Biamonte, J.; Wittek, P.; Pancotti, N.; Rebentrost, P.; Wiebe, N.; Lloyd, S. Quantum machine learning. *Nature* **2017**, *549*, 195.

(20) Havlíček, V.; Córcoles, A. D.; Temme, K.; Harrow, A. W.; Kandala, A.; Chow, J. M.; Gambetta, J. M. Supervised learning with quantum-enhanced feature spaces. *Nature* **2019**, *567*, 209.

(21) Ginzburg, P.; Berkovitch, N.; Nevet, A.; Shor, I.; Orenstein, M. Resonances on-demand for plasmonic nano-particles. *Nano Letters* **2011**, *11*, 2329–2333.

(22) Forestiere, C.; Pasquale, A. J.; Capretti, A.; Miano, G.; Tamburrino, A.; Lee, S. Y.; Reinhard, B. M.; Dal Negro, L. Genetically engineered plasmonic nanoarrays. *Nano Letters* **2012**, *12*, 2037–2044.

(23) Feichtner, T.; Selig, O.; Kiunke, M.; Hecht, B. Evolutionary optimization of optical antennas. *Phys. Rev. Lett.* **2012**, *109*, 127701.

(24) Feichtner, T.; Selig, O.; Hecht, B. Plasmonic nanoantenna design and fabrication based on evolutionary optimization. *Optics Express* **2017**, *25*, 10828–10842.

(25) Mirzaei, A.; Miroshnichenko, A. E.; Shadrivov, I. V.; Kivshar, Y. S. Superscattering of light optimized by a genetic algorithm. *Applied Physics Letters* **2014**, *105*, 011109.

(26) Wiecha, P. R.; Arbouet, A.; Girard, C.; Lecestre, A.; Larrieu, G.; Paillard, V. Evolutionary multi-objective optimization of colour pixels based on dielectric nanoantennas. *Nature Nanotechnology* **2017**, *12*, 163.

(27) Johlin, E.; Mann, S. A.; Kasture, S.; Koenderink, A. F.; Garnett, E. C. Broadband highly directive 3D nanophotonic lenses. *Nature Communications* **2018**, *9*, 4742.

(28) Ma, W.; Cheng, F.; Liu, Y. Deep-learning-enabled on-demand design of chiral metamaterials. *ACS Nano* **2018**, *12*, 6326–6334.

(29) Sajedian, I.; Badloe, T.; Rho, J. Optimisation of colour generation from dielectric nanostructures using reinforcement learning. *Optics Express* **2019**, *27*, 5874–5883.

(30) Jiang, J.; Fan, J. A. Global optimization of dielectric metasurfaces using a physics-driven neural network. *Nano Lett.* **2019**, *19*, 5366–5372.

(31) Li, Y.; Xu, Y.; Jiang, M.; Li, B.; Han, T.; Chi, C.; Lin, F.; Shen, B.; Zhu, X.; Lai, L.; Fang, Z. Self-Learning Perfect Optical Chirality via a Deep Neural Network. *Phys. Rev. Lett.* **2019**, *123*, 213902.

(32) Liu, Z.; Yan, S.; Liu, H.; Chen, X. Superhigh-Resolution Recognition of Optical Vortex Modes Assisted by a Deep-Learning Method. *Phys. Rev. Lett.* **2019**, *123*, 183902.

(33) Wiecha, P. R.; Muskens, O. L. Deep learning meets nanophotonics: A generalized accurate predictor for near fields and far fields of arbitrary 3D nanostructures. *Nano Letters* **2019**, *20*, 329–338.

(34) Melati, D.; Grinberg, Y.; Dezfouli, M. K.; Janz, S.; Cheben, P.; Schmid, J. H.; Sánchez-Postigo, A.; Xu, D.-X. Mapping the global design space of nanophotonic components using machine learning pattern recognition. *Nature Communications* **2019**, *10*, 4775.

(35) Wiecha, P. R.; Lecestre, A.; Mallet, N.; Larrieu, G. Pushing the limits of optical information storage using deep learning. *Nature Nanotechnology* **2019**, *14*, 237.

(36) Liu, Z.; Liu, X.; Xiao, Z.; Lu, C.; Wang, H.-Q.; Wu, Y.; Hu, X.; Liu, Y.-C.; Zhang, H.; Zhang, X. Integrated nanophotonic wavelength router based on an intelligent algorithm. *Optica* **2019**, *6*, 1367–1373.

(37) Jin, Z.; Mei, S.; Chen, S.; Li, Y.; Zhang, C.; He, Y.; Yu, X.; Yu, C.; Yang, J. K.; Lukýanchuk, B.; Xiao, S.; Qiu, C.-W. Complex Inverse Design of Meta-optics by Segmented Hierarchical Evolutionary Algorithm. *ACS Nano* **2019**, *13*, 821–829.

(38) Bonod, N.; Bidault, S.; Burr, G. W.; Mivelle, M. Evolutionary Optimization of All-Dielectric Magnetic Nanoantennas. *Advanced Optical Materials* **2019**, *7*, 1900121.

(39) Li, Z.; Rosenmann, D.; Czaplewski, D. A.; Yang, X.; Gao, J. Strong circular dichroism in chiral plasmonic metasurfaces optimized by micro-genetic algorithm. *Optics Express* **2019**, *27*, 28313–28323.

(40) Jiang, J.; Sell, D.; Hoyer, S.; Hickey, J.; Yang, J.; Fan, J. A. Free-form diffractive metagrating design based on generative adversarial networks. *ACS Nano* **2019**, *13*, 8872–8878.

(41) Gao, L.; Li, X.; Liu, D.; Wang, L.; Yu, Z. A Bidirectional Deep Neural Network for Accurate Silicon Color Design. *Advanced Materials* **2019**, *31*, 1905467.

(42) Liu, Z.; Zhu, D.; Lee, K.-T.; Kim, A. S.; Raju, L.; Cai, W. Compounding Meta-Atoms into Metamolecules with Hybrid Artificial Intelligence Techniques. *Advanced Materials* **2019**, *31*, 1904790.

(43) Ma, W.; Cheng, F.; Xu, Y.; Wen, Q.; Liu, Y. Probabilistic representation and inverse design of metamaterials based on a deep generative model with semi-supervised learning strategy. *Advanced Materials* **2019**, *31*, 1901111.

(44) Coello, C. A. C.; Lamont, G. B.; Van Veldhuizen, D. A. *Evolutionary algorithms for solving multi-objective problems*; Springer: Berlin, Germany, 2007; Vol. 5.

(45) Tao, P.; Ni, G.; Song, C.; Shang, W.; Wu, J.; Zhu, J.; Chen, G.; Deng, T. Solar-driven interfacial evaporation. *Nature Energy* **2018**, *3*, 1031–1041.

(46) Zhang, X.; Chen, Y. L.; Liu, R.-S.; Tsai, D. P. Plasmonic photocatalysis. *Reports on Progress in Physics* **2013**, *76*, 046401.

(47) Aubry, A.; Lei, D. Y.; Fernández-Domínguez, A. I.; Sonnefraud, Y.; Maier, S. A.; Pendry, J. B. Plasmonic light-harvesting devices over the whole visible spectrum. *Nano Letters* **2010**, *10*, 2574–2579.

(48) Lei, D. Y.; Aubry, A.; Maier, S. A.; Pendry, J. B. Broadband nano-focusing of light using kissing nanowires. *New Journal of Physics* **2010**, *12*, 093030.

(49) Lei, D. Y.; Aubry, A.; Luo, Y.; Maier, S. A.; Pendry, J. B. Plasmonic interaction between overlapping nanowires. *ACS Nano* **2010**, *5*, 597–607.

(50) Aubry, A.; Lei, D. Y.; Maier, S. A.; Pendry, J. Interaction between plasmonic nanoparticles revisited with transformation optics. *Phys. Rev. Lett.* **2010**, *105*, 233901.

(51) Wyszecki, G.; Stiles, W. S. *Color science*; Wiley New York, 1982; Vol. 8.

(52) Pors, A.; Nielsen, M. G.; Della Valle, G.; Willatzen, M.; Albrektsen, O.; Bozhevolnyi, S. I. Plasmonic metamaterial wave retarders in reflection by orthogonally oriented detuned electrical dipoles. *Optics Letters* **2011**, *36*, 1626–1628.

(53) Tan, S. J.; Zhang, L.; Zhu, D.; Goh, X. M.; Wang, Y. M.; Kumar, K.; Qiu, C.-W.; Yang, J. K. Plasmonic color palettes for photorealistic printing with aluminum nanostructures. *Nano Letters* **2014**, *14*, 4023–4029.

(54) Guo, X.; Ding, Y.; Duan, Y.; Ni, X. Nonreciprocal Metasurface with Space-Time Phase Modulation. *Light: Science & Applications* **2019**, *8*, 123.

(55) Dong, Z.; Ho, J.; Yu, Y. F.; Fu, Y. H.; Paniagua-Dominguez, R.; Wang, S.; Kuznetsov, A. I.; Yang, J. K. Printing beyond sRGB color gamut by mimicking silicon nanostructures in free-space. *Nano Letters* **2017**, *17*, 7620–7628.

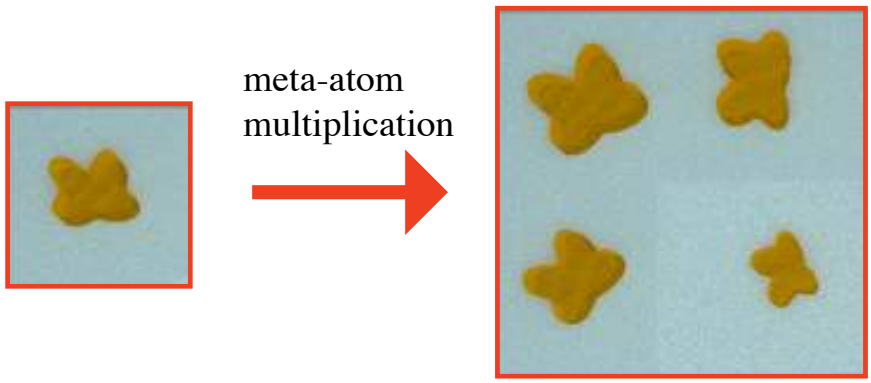

Figure 1: Concept of meta-atom multiplication. (a) A schematic of a photonic structure with unextended unit cell. Only one meta-atom inside the unit cell (red box). (b) A schematic of a photonic structure with extended unit cell. Four meta-atoms in one unit cell with different size, position and orientation, drastically enlarging the parameter space for optimised performance.

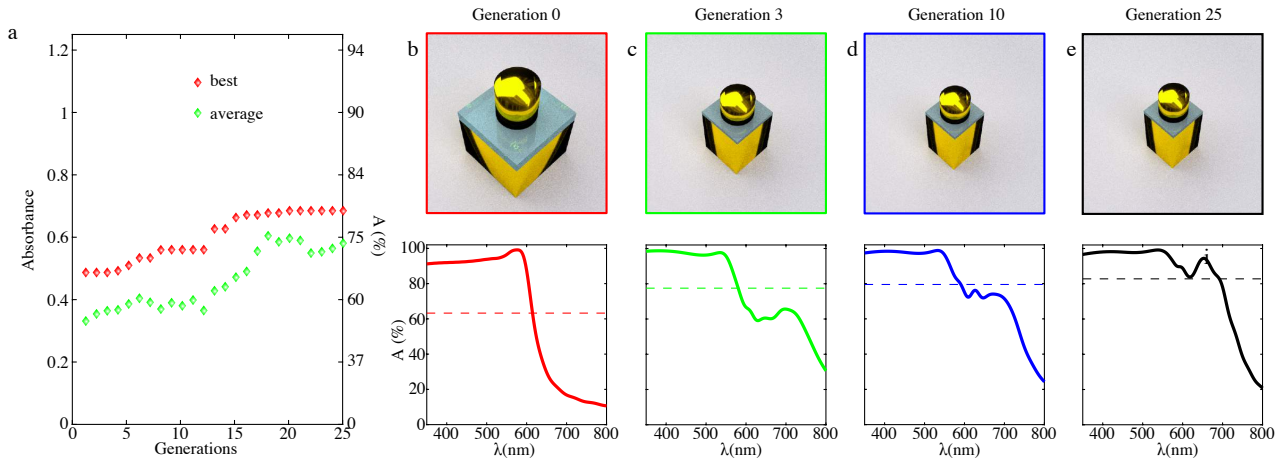

Figure 2: GA-based optimisation for broadband absorption with unextended unit cell composed of a single meta-atom. (a) Relationship between the number of generations and absorption averaged between 350nm to 800nm ($\bar{A}$). Both best values (red diamonds) and averaged value (green diamonds) in each generation are demonstrated. (b-e) Details of best configurations in different generations. Upper panel shows a schematic of the configuration and lower panel shows the absorption spectrum. Dashed line corresponds to the value of $\bar{A}$. For quantitate parameters refer to Supporting Information 2.

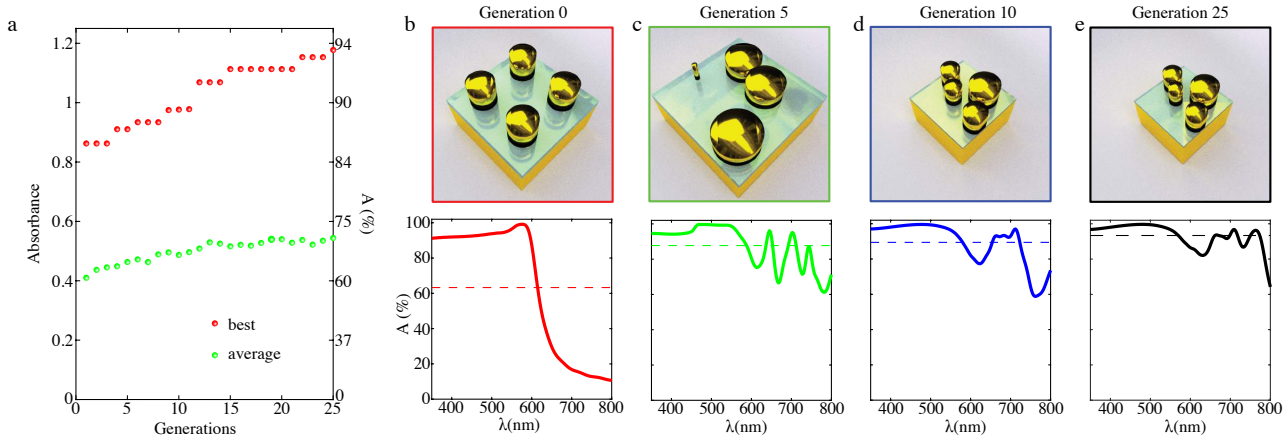

Figure 3: GA-based optimisation for broadband absorption with extended unit cell composed of four different meta-atoms. (a) Relationship between the number of generations and absorption averaged between 350nm to 800nm ($\bar{A}$). Both best values (red circles) and averaged value (green circles) in each generation are demonstrated. (b-e) Details of best configurations in different generations. Upper panel shows a schematic of the configuration and lower panel shows the absorption spectrum. Dashed line corresponds to the value of $\bar{A}$. For quantitate parameters refer to Supporting Information 2.

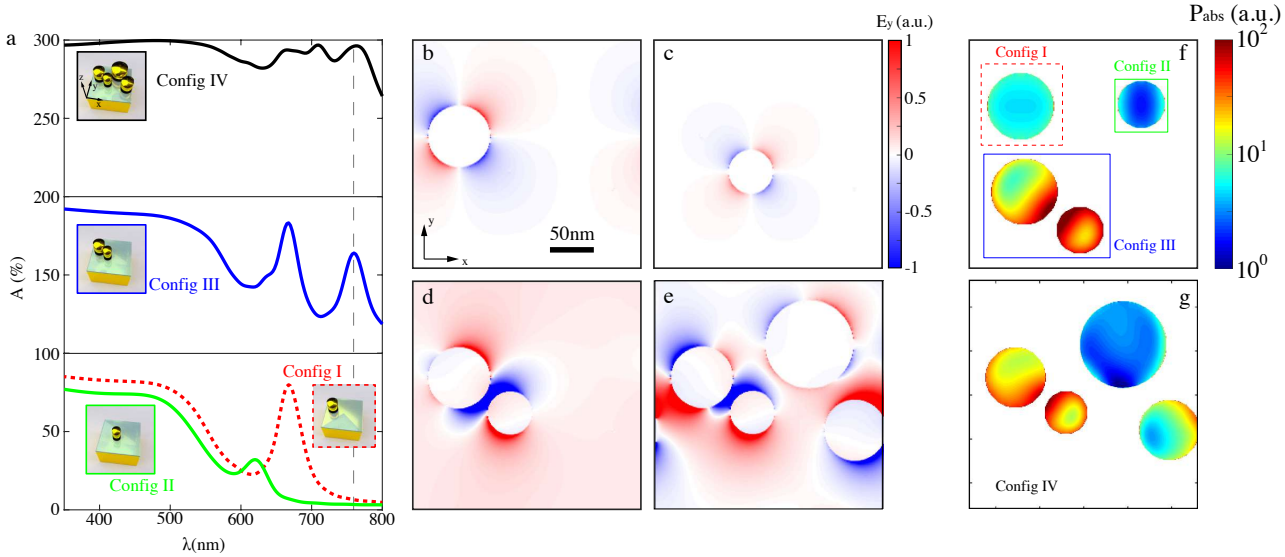

Figure 4: Analysis of the extended unit cell with optimised absorption. (a) Absorption spectra of different configurations. Upper panel: spectrum from the configuration with all four disks. Middle panel: spectrum from the configuration with only two (out of four) disks. Lower panel: spectra from the configurations with a single disk. The schematic cartoon for the configuration is demonstrated as inset for each panel. (b-e) Spatial distribution of electric field E_y for the four configurations in a): b) Config I; c) Config II; d) Config III; e) Config IV. (f-g) The spatial distribution of absorption power density P_{abs} inside disks: f) Config I, Config II and Config III; g) Config IV. The wavelength is 760nm in (b-g).

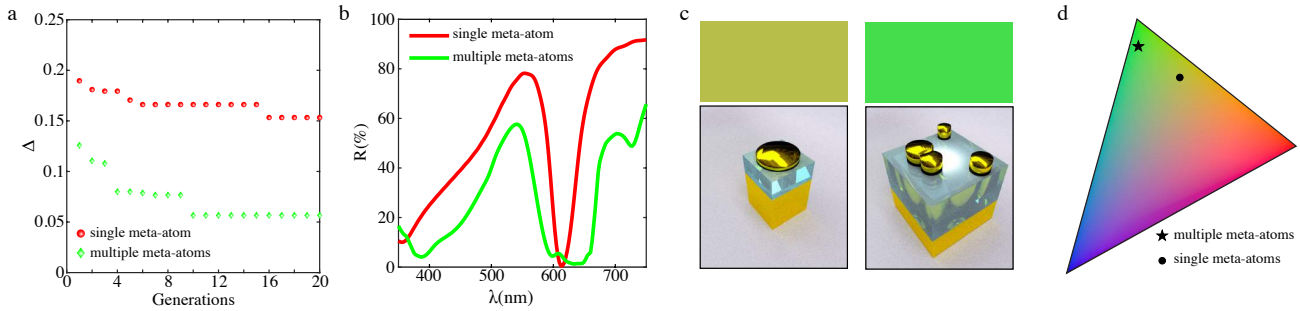

Figure 5: GA based optimisation for the structural colour generation. The aim is the green colour of sRGB. (a) The distance Δ between the target colour and the structural colour generated in the CIE diagram as a function of generations. Red circles represent the unextended unit cell while green diamonds represent the unit cell after meta-atom multiplicaiton. (b) A comparison of reflection spectra between the optimised samples of unextended (green) and extended (red) unit cells. (c) A comparison of generated colours and corresponding configurations. The left column is for the case with single meta-atom while the right column is for the case with multiple meta-atoms. For quantitate parameters refer to Supporting Information 3. (d)The generated colours in the CIE diagram, circle for single meta-atom case and pentagram for multiple meta-atom case.

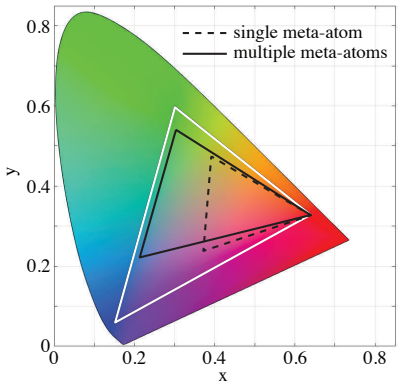

Figure 6: A comparison of colour coverage in CIE diagram for unextended unit cell with single meta-atom (black dashed line) and extended unit cell with multiple meta-atoms (black line). The sRBG space is enclosed inside the white triangle.

Graphical TOC Entry

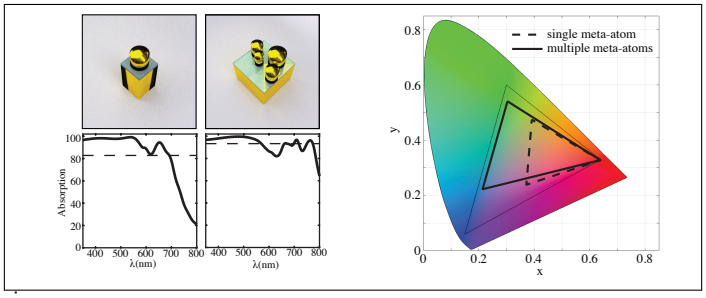

:

Genetic-algorithm-aided meta-atom multiplication for improved absorption and colouration in nanophotonics
Changxu Liu, Stefan A. Maier, Guxin Li
By utilising the genetic algorithm as an optimiser, enhanced broadband absorption and improved structural colour generation can be achieved through the multiplication of meta-atoms in the unit cell.